

# LEVERAGING THE CONTINUOUS ADJOINT METHOD FOR INDUSTRIAL SCALE APPLICATION

Georgios K. Karpouzas, Dr. Eugene de Villiers  
ENGYS Ltd, United Kingdom

Dr. Daniel P. Combest  
ENGYS LLC, United States

## 1. Introduction

One of the fastest growing fields in CFD research is adjoint optimization. Adjoint methods are widely used from people in industry to optimize their products [1]. Drag force minimization of a car, lift force maximization of aeroplanes and minimization of power losses in ducts are some of these optimization problems.

The adjoint method provides the sensitivity derivatives of the objective function (drag force etc.) with respect to the design variables (nodal displacement towards the normal direction of the surface). The calculation of the sensitivity derivatives is independent from the number of the design variables which gives the adjoint method a major advantage comparing with the other methods, especially in the problems with large design spaces.

There are two kinds of adjoint methods: the discrete and the continuous. In the discrete approach, the discretization precedes the differentiation. In this case, a manual or automatic differentiation (using a tool like TAPENADE) is performed in the base CFD source code. In the continuous approach, the adjoint equations are formulated, after the differentiation of the analytic flow equations (primal problem). Then, the adjoint equations are discretized and solved. Applying the two approaches in simple cases, the calculation of the sensitivity derivatives is fast, easy and straight-forward. However, in industrial scale applications the solution of the adjoint problem is complicated. The discrete adjoint can theoretically provide the “exact” gradient but requires large amount of memory and computational cost. More precisely, all the intermediate variables have to be stored in the memory. In discrete terminology these variables are called “tape”. Techniques such as revolve (check-pointing) have developed to reduce the memory requirements but this increases the computational cost. In the continuous adjoint method, the differentiation of the analytical primal flow equations

can be complicated and time-consuming. This depends from the complexity of the primal equations but it happens once. The memory requirements and computational cost is similar with the solution of the primal equations, which makes it very useful tool for high resolution meshes. In some cases, adjoint problem can be ill-posed and difficult to solve. In the continuous approach, the instabilities can be easily identified and corrected because the adjoint equations have already been formulated, whereas in the discrete approach any correction inside the code can be complicated.

In this paper, we demonstrate the use of the continuous adjoint method for shape and topology optimization problems. The primal flow equations are the steady-state RANS (Reynolds-Averaged-Navier-Stokes).

$$\begin{aligned}
R^p &= \frac{\partial v_j}{\partial x_j} = 0 \\
R_i^v &= v_j \frac{\partial v_i}{\partial x_j} + \frac{\partial p}{\partial x_j} - \frac{\partial}{\partial x_j} \left[ (nu + nu_t) \left( \frac{\partial v_i}{\partial x_j} + \frac{\partial v_j}{\partial x_i} \right) \right] = 0 \\
R_i^z &= \text{Convection} + \text{Diffusion} + \text{Production} + \text{Dissipation} = 0
\end{aligned} \tag{1}$$

Where  $v_i$  is the primal velocity,  $p$  is the primal pressure,  $nu$  and  $nu_t$  are the kinematic and turbulent kinematic viscosity, respectively.  $R_z$  is considered to be an arbitrary turbulence model and  $z_i$  represents the turbulence variable. The objective function  $F$  can be defined on the surface and volume integral.  $F$  is extended by the state equations,  $R_p$  and  $R_{v_i}$ . The variables  $q$  and  $u_i$  are the adjoint pressure and adjoint velocity respectively. In this paper, the turbulent kinematic viscosity  $nu_t$  is assumed frozen (frozen turbulence assumption).

$$F = \int_s F_s dS + \int_{\Omega} F_{\Omega} d\Omega \tag{2}$$

$$F_{aug} = F + \int_{\Omega} q R^p d\Omega + \int_{\Omega} u_i R_i^v d\Omega \tag{3}$$

After differentiating the  $F_{aug}$  (see Appendix (5) for details), the adjoint equations (eq. (4)) appear.

## LEVERAGING THE CONTINUOUS ADJOINT METHOD FOR INDUSTRIAL SCALE APPLICATION

$$R_{\Omega}^q = \frac{\partial u_j}{\partial x_j} - \frac{\partial F}{\partial p} = 0$$

$$R_{i\Omega}^u = -v_j \frac{\partial u_i}{\partial x_j} + u_j \frac{\partial v_j}{\partial x_i} + \frac{\partial q}{\partial x_j} - \frac{\partial}{\partial x_j} \left[ (nu + nu_t) \left( \frac{\partial u_i}{\partial x_j} + \frac{\partial u_j}{\partial x_i} \right) \right] + \frac{\partial F}{\partial v_i} = 0$$
(4)

Where  $u_i$  and  $q$  are the adjoint velocity and pressure respectively. The adjoint equations are very similar with the primal equations (eq. (1)). They both have a convection, a diffusion, a gradient of pressure and a source term. The only difference is the additional term  $(u_j \frac{\partial v_j}{\partial x_i})$ , which is appeared in the adjoint momentum equations. This term is called ATC (Adjoint Transpose Convection) and it is the source of any instabilities in the solution of the adjoint problem. The ATC term can be alternatively written as  $-v_j \frac{\partial u_j}{\partial x_i}$  (using one more Green-Gauss theorem).

After solving the adjoint equations, the surface sensitivities are calculated with the following expression:

$$\frac{\delta F_{aug}}{\delta b} = - \int_{S_w} \left[ (nu + nu_t) \left( \frac{\partial u_i}{\partial x_j} + \frac{\partial u_j}{\partial x_i} \right) - qn_i \right] \frac{\partial v_i}{\partial x_k} \frac{\delta x_k}{\delta b_m} dS$$
(5)

In shape optimization problems, the surface sensitivities are used as an input to a deformation tool which morphs the computational domain. In cases with large deformations, the morphing tool usually fails to produce valid mesh and re-meshing is required. As a result, the primal and adjoint equations have to be solved from scratch which increases the computational cost.

In topology optimization problems, a new method which couples the adjoint method with level-set and immersed boundaries is used. In the level-set method, the interface is tracked by the level-set variable  $\phi$ , which is the signed distance from interface (Figure 1). The level-set method is inspired from a paper of J.A. Sethian [3] and constitutes three parts: velocity extension, evolution and reinitialisation.

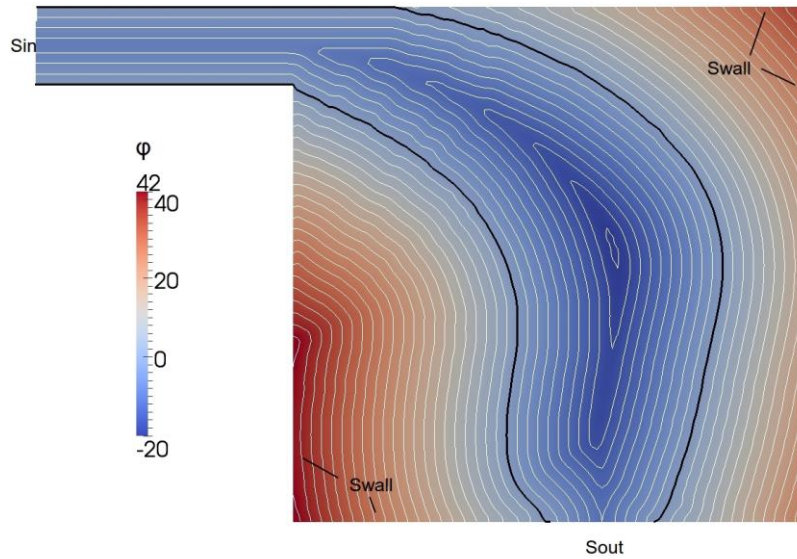


Figure 1. This figure represents the level-set Field. The zero level-set field represents the interface.

In first stage, the sensitivity derivatives are calculated on the interface using the continuous adjoint method. Then, the velocity extension equation is used to extend the sensitivities towards the normal direction of the interface. The interface is evolved by solving a Hamilton-Jacobi equation (level-set equation). After the evolution, the level-set field is not a distance field anymore. As a result, the level-set field must be corrected by solving the reinitialisation equation. Immersed boundaries have developed and used on the zero level-set field to model accurately the interface as a wall boundary.

## 2. Applications

The presented method is developed in a plugin of HELYX called adjointFoam. In this section, three industrial cases are presented:

- Topology optimization of a HVAC duct.
- Topology optimization of a gear pump.
- One-step shape optimization of the DRIVAER estate car.

## LEVERAGING THE CONTINUOUS ADJOINT METHOD FOR INDUSTRIAL SCALE APPLICATION

In the first application, topology optimization of a HVAC cooling duct (Figure 2) is presented.

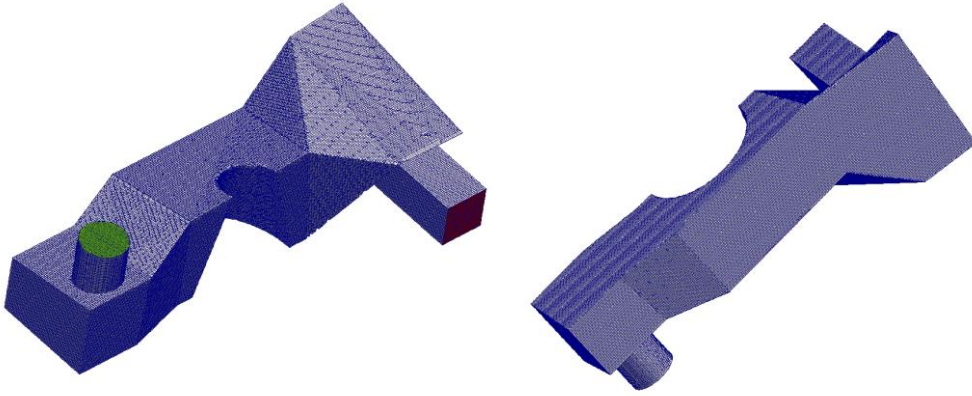


*Figure 2. In these figures the baseline mesh of the duct is presented. The inlet and the outlet boundaries are the red and green patches, respectively. The mesh is generated using hex-dominant mesh generator (helyxHexMesh) and has 600.694 cells.*

The red and green patch is the inlet and the outlet respectively. The fluid is air and the boundary conditions are:

- Inlet flow rate is  $m = 0.0133$  kg/s.
- Outlet pressure is  $p = 0$  Pa.

The reduction of the power loss between the inlet and the outlet is chosen for an objective function.

$$F = -\int_{S_{io}} \left( p + \frac{1}{2} \rho v^2 \right) v_i n_i dS$$

(6)

The continuous adjoint method coupled with level set and immersed boundaries is used. After the optimization, the objective was reduced by ~50%. The optimized surfaces and the velocity streamlines are shown in Figure 3 and Figure 4, respectively.

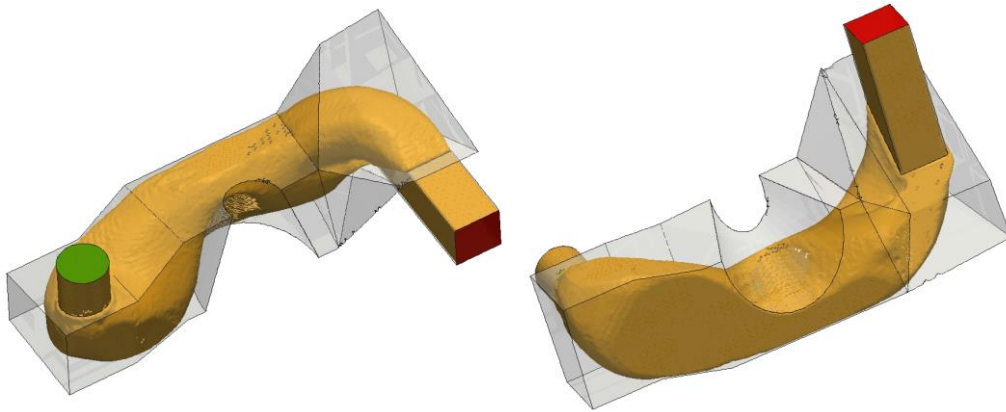


Figure 3. This picture represents the baseline geometry (grey box) and the optimized geometry (yellow surface). The optimized surface (zero level-set field) can be directly extracted to an stl format.

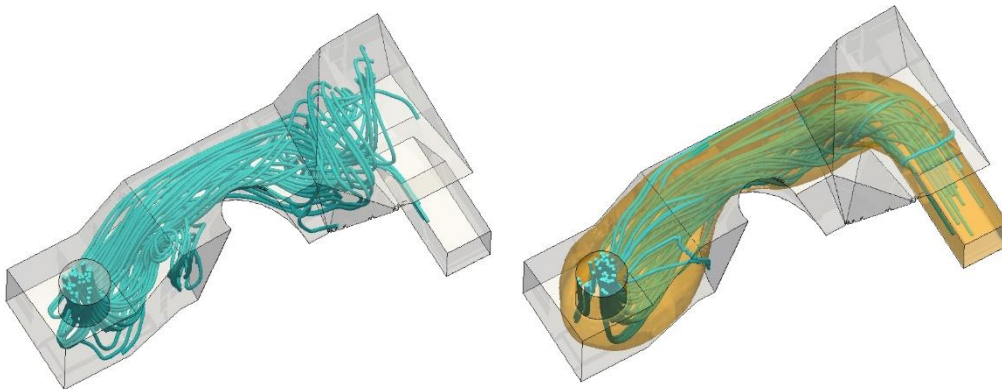


Figure 4. Velocity streamlines before (left) and after (right) the optimization.

## LEVERAGING THE CONTINUOUS ADJOINT METHOD FOR INDUSTRIAL SCALE APPLICATION

In the second application, the power losses of a gear pump (Figure 5) are minimized. The gear pump geometry is provided by the Aisin AW Company.

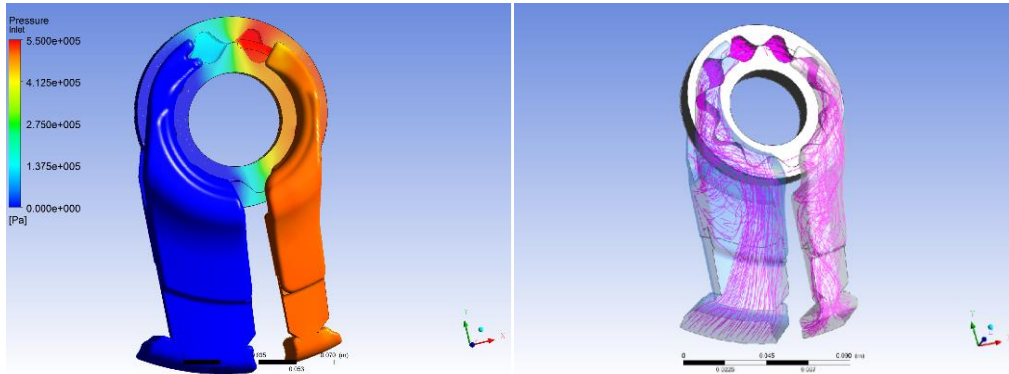


Figure 5. This figure represents the whole gear pump (inport, gear and output). The recirculation areas indicate that the power losses can be optimized.

The geometry is split into two different cases, which are presented in Figure 6. The fluid is a lubricant oil with kinematic viscosity  $\nu=1.09047 \times 10^{-5} \text{m}^2/\text{s}$  and density  $\rho=829 \text{kg/m}^3$ .

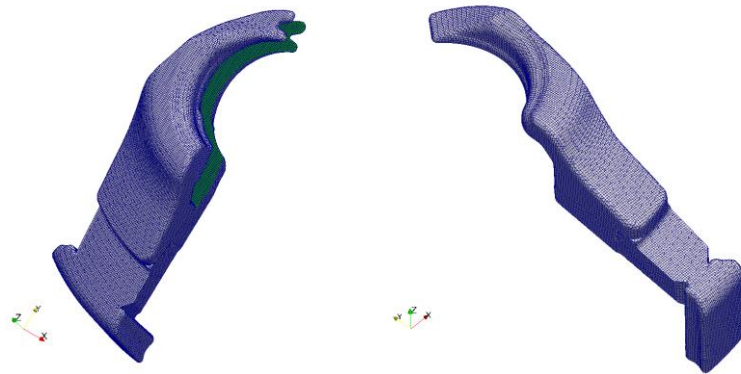


Figure 6. In this figure, the mesh for the inport (left) and output (right) ducts, generated with the helyxHexMesh mesh generator, is presented. The mesh size for the inport and output is 330000 and 175000 cells, respectively.

The primal problem has the following boundary conditions:

- Inlet port boundaries:
  - The mass flow at each outlet is  $\dot{m}=0.375 \text{kg/s}$ .
  - Inlet pressure:  $p=0 \text{Pa}$ .

- Outlet port boundaries:
  - Inlet mass flow:  $\dot{m} = 0.75 \text{ kg/s}$ .
  - Outlet pressure:  $p = 500 \text{ kPa}$ .

The continuous adjoint method coupled with level-set and immersed boundaries was chosen to minimize the power losses for each of the two ducts. The optimized surfaces and the velocity streamlines are shown on Figure 7 and Figure 8, respectively. After the optimization, the power losses were decreased by  $\sim 19\%$  (Table 1: ).

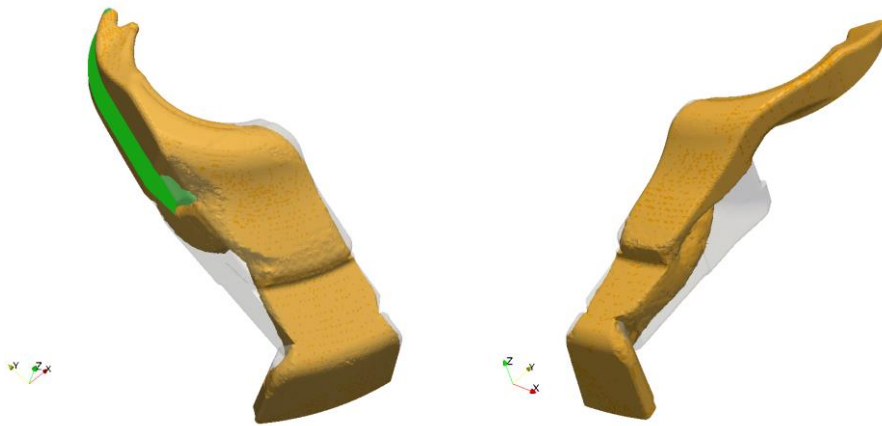


Figure 7. This figure represents the optimized shapes. The orange surface is the zero level set field, whereas the transparent grey surface consists the baseline mesh.



Figure 8. The left and right figure represents the streamlines for the baseline and optimized ducts. The optimization was clearly successful as the recirculation zones have all but disappeared.

## LEVERAGING THE CONTINUOUS ADJOINT METHOD FOR INDUSTRIAL SCALE APPLICATION

	Inport	Outport	Gearpump
<b>Baseline(W)</b>	2.308	31.017	33.325
<b>Optimized(W)</b>	1.635	25.379	27.013
<b>%</b>	29.17	18.18	18.94

**Table 1: Objective function values before and after optimization. The power losses of the gear pump decreased by about 18.94%.**

In the third application, drag sensitivities are calculated on the DRIVAER estate car. The objective function for drag reduction has the following expression:

$$F = -\int_{S_w} \left( nu \left( \frac{\partial v_i}{\partial x_j} + \frac{\partial v_j}{\partial x_i} \right) - p \delta_i^j \right) n_j r_i dS \quad (7)$$

Where the  $r_i$  is the drag direction.

The mesh is generated with the helyxHexMesh and it has ~35 million cells (Figure 9).

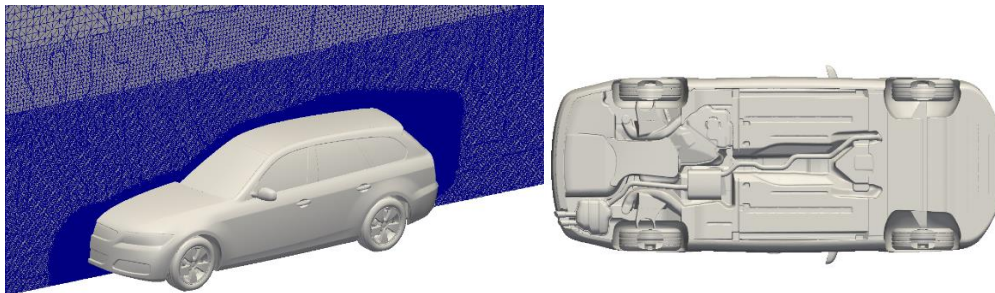


*Figure 9. This figure represents the DRIVAER estate mesh generated with helyxHexMesh. The geometry is asymmetric and the underbody is fully detailed. Geometry provided by [5].*

The fluid is air with kinematic viscosity  $\nu=1,5881 \times 10^{-5} \text{m}^2/\text{s}$  and density  $\rho=1,205 \text{ kg/m}^3$ . The RANS flow equations are used for the primal problem. The freestream velocity is set to  $v=140 \text{ km/h}$ . The Spalart-Allmaras turbulent model is chosen, as the flow is turbulent.

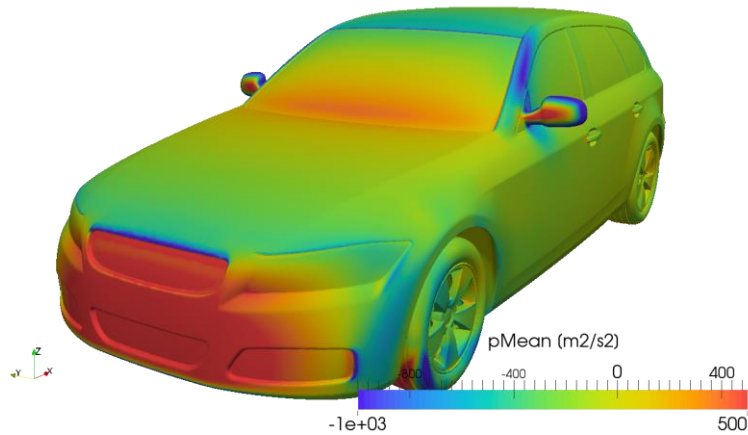


Figure 10. Primal pressure Field

After solving the adjoint equations, the drag sensitivities are calculated and represented in Figure 11. Based on these sensitivities, a single optimization step is performed to reduce the drag force. The drag coefficient in the baseline mesh was  $C_d=0.356$ . The new  $C_d$ , after one optimization step based on the calculated drag sensitivities, is reduced by 28 counts ( $C_d=0.328$ , 7.8% drag reduction).

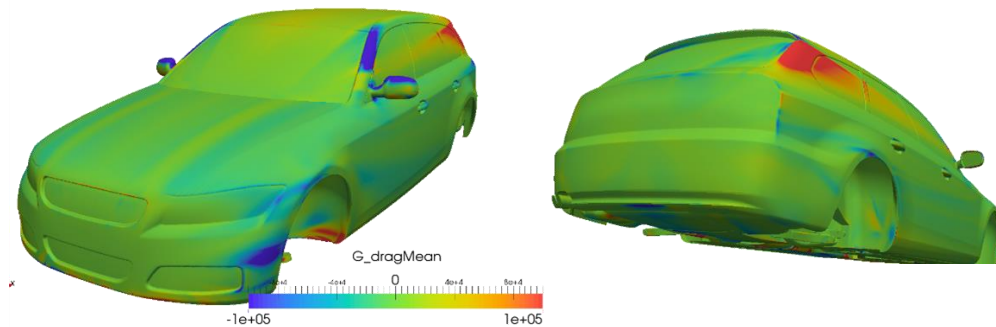


Figure 11. These pictures represent the drag sensitivities. The drag force will be reduced if the regions with blue and red colour will be pushed in and out respectively.

## LEVERAGING THE CONTINUOUS ADJOINT METHOD FOR INDUSTRIAL SCALE APPLICATION

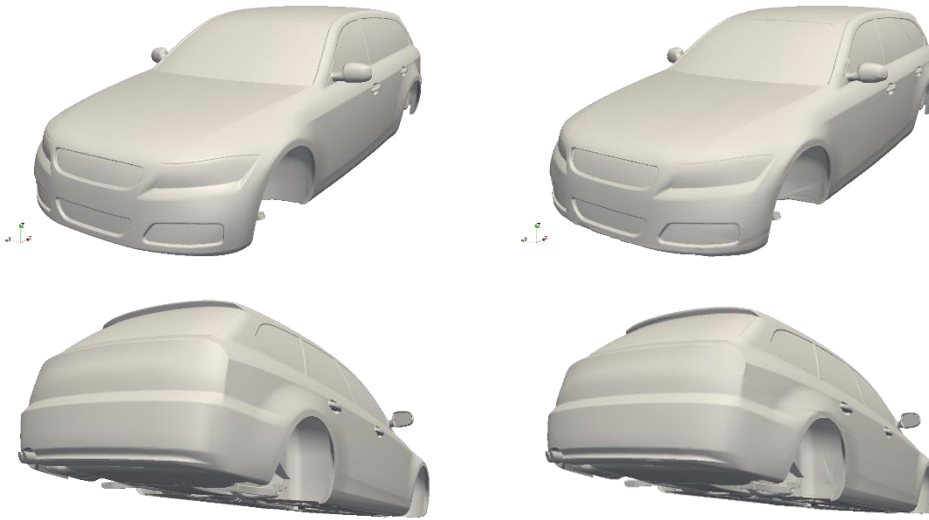


Figure 12 Car geometry before (left) and after (right) the one optimization step.

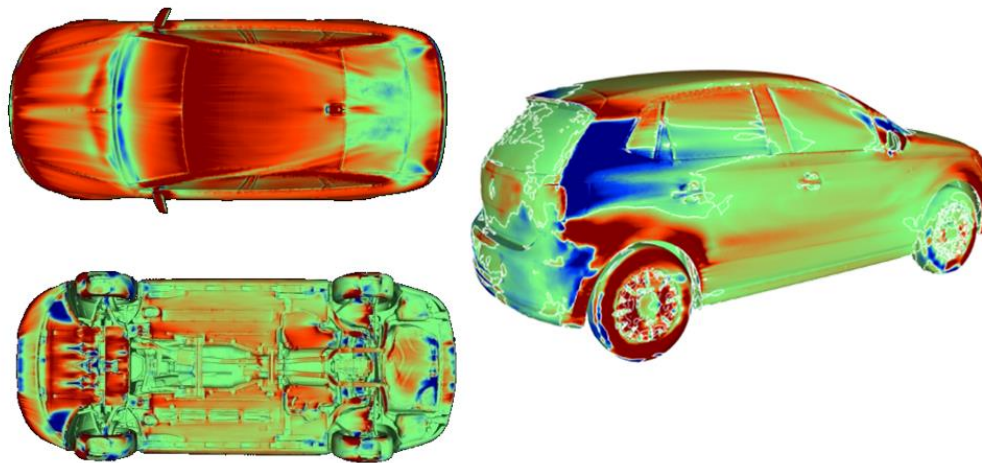


Figure 13 Sensitivity maps to reduce drag force in various industrial scale applications. Images taken from C.Othmer paper [1].

### 3. Summary

In this paper, the continuous adjoint method used for shape and topology optimization problems, is presented. The presented methodology is over and over tested and worked from the industry with high resolution meshes. The huge advantage of the method is that calculation of the sensitivity derivatives requires similar memory and computational cost as the solution of the primal problem. As a result, the continuous adjoint

method is a powerful tool for optimization, especially in large scale applications. Moreover, it is possible to use a DES turbulent model in the primal problem. This can lead to better accuracy in the sensitivity derivatives as the accuracy in the primal problem is improved (see [1]). Finally, the continuous adjoint method can also be extended in other applications, like aeroacoustics, CHT, passive scalar transport etc..

#### 4. References

[1] Othmer C. 2014. *Adjoint methods for car aerodynamics*. Journal of Mathematics in Industry 4:6

[2] Zymaris A.S., Papadimitriou D.I., Giannakoglou K.C., Othmer C. 2010. *Adjoint wall functions: A new concept for use aerodynamic shape optimization*. Journal of Computational Physics, 229:5528–5245

[3] Sethian J.A. 2001. *Evolution, implementation, and application of level set and fast marching methods for advancing fronts*. Journal of Computational Physics, 169:503–555.

[4] Karpouzas G.K., De Villiers E. 2014. *Level-set based topology optimization using the continuous adjoint method*. An International Conference on Engineering and Applied Sciences Optimization. OPT-I 2014

[5] A. I. Heft, T. Indinger, N. A. Adams. 2012. *Introduction of a New Realistic Generic Car Model for Aerodynamic Investigations*. SAE 2012 World Congress, Detroit, Michigan, USA, Paper 2012-01-1068

# LEVERAGING THE CONTINUOUS ADJOINT METHOD FOR INDUSTRIAL SCALE APPLICATION

## 5. Appendix

The objective function  $F$  can be defined on the surface and volume integral.  $F$  is extended by the state equations,  $R_p$  and  $R_{vi}$ . The variables  $q$  and  $u_i$  are the adjoint pressure and adjoint velocity respectively. The turbulent kinematic viscosity  $\nu_t$  is assumed frozen (frozen turbulence assumption).

$$F = \int_s F_s dS + \int_{\Omega} F_{\Omega} d\Omega \quad (8)$$

$$F_{aug} = F + \int_{\Omega} q R^p d\Omega + \int_{\Omega} u_i R_i^v d\Omega \quad (9)$$

Using the Leibnitz theorem, the variation of the augmented objective function is:

$$\frac{\delta F_{aug}}{\delta b} = \frac{\delta F}{\delta b} + \int_{\Omega} q \frac{\partial R^p}{\partial b} d\Omega + \int_{\Omega} u_i \frac{\partial R_i^v}{\partial b} d\Omega + \int_s (u_i R_i^v + q R^p) \frac{\delta x_k}{\delta b} n_k dS \quad (10)$$

After expanding the  $R_{vi}$  and  $R_p$  terms, the  $\frac{\partial v_i}{\partial b}$  and  $\frac{\partial p}{\partial b}$  terms appear. The computational cost of these terms is extremely high because their calculation is depended from the number of mesh cells. The adjoint method formulates the expressions using the Green-Gauss theorem and the multipliers of these terms are forced to become zero. As a result, the calculation of these terms is avoided.

$$\frac{\delta F_{aug}}{\delta b} = \int_{\Omega} R_i^u \frac{\partial v_i}{\partial b} d\Omega + \int_s R_i^u \frac{\partial v_i}{\partial b} dS + \int_{\Omega} R_{\Omega}^q \frac{\partial p}{\partial b} d\Omega + \int_s R_s^q \frac{\partial p}{\partial b} dS + G(u, v, q, p) \quad (11)$$

Where the  $R_u$  and  $R_q$  in the volume and surface integral are the adjoint equations and their boundary conditions respectively.